Reduction of Cogging Torque in AFPM Machine Using Elliptical-Trapezoidal-Shaped Permanent Magnet

S. Ali [1], J. Ikram [1], C. P. Devereux [2], S. S. H. Bukhari [3,4*], S. A. Khan [1], N. Khan [1], and J.-S. Ro [3,5*]

[1] Department of Electrical and Computer Engineering, COMSATS University Islamabad, Islamabad, Pakistan

[2] Research and Development Lab. Omnidex Group Limited, Guangzhou 510050, P.R. China

[3] School of Electrical and Electronics Engineering, Chung-Ang University, Seoul, South Korea

[4] Department of Electrical Engineering, Sukkur IBA University, Sukkur, Sindh, Pakistan

[5] Department of Intelligent Energy and Industry, Chung-Ang University, Seoul, South Korea
*jongsukro@gmail.com, *sabir@iba-suk.edu.pk

Abstract ─ The reduction in cogging torque enables smooth operation and an increase in the torque density of the machine. This research aims to minimize cogging torque in dual rotor single stator axial flux permanent magnet (AFPM) machine. Reduction in cogging torque makes the back EMF sinusoidal and reduces the torque ripples in AFPM machine. In this paper, an elliptical trapezoidal-shaped permanent magnet (PM) is proposed to minimize torque ripples of the AFPM machine. The 3D finite element analysis (FEA) is used for the analysis of AFPM machine. The optimization of AFPM machine is done by employing the asymmetric magnet-overhang along with the parameters of elliptical-shaped PM using Genetic algorithm (GA).

Index Terms ─ Axial flux machine, cogging torque, elliptical-trapezoidal magnet, FEA, slot-less, torque ripples.

I. INTRODUCTION

Axial flux permanent magnet (AFPM) machines are getting popularity for electric vehicle and wind energy system, nowadays [1]–[2]. AFPM machines are beneficial as compared to radial flux machines due to higher torque and power density because of their high D/L ratio [2]–[4]. Furthermore, AFPM machine are suitable for low-speed direct drive applications since it can accommodate large number of poles. In addition, it is feasible due to its adjustable air-gap capability. Moreover, AFPM machine has high torque characteristics at low speed without utilizing mechanical gearbox. It is worth noted that slotless AFPM machine has less torque ripples as compared to the slotted AFPM machines. To further, dual rotor slotless AFPM machine has balanced magnetic force as compared to a single rotor AFPM machine. Due to higher D/L ratio, end winding in AFMs is smaller with drum type winding configuration as compared to the ring type winding configuration. In drum winding, for slotless dual rotor AFPM machine, only N-N magnet configuration is used [5]–[9].

Different techniques are used to minimize the torque ripples, *i.e.*, change in the shape of magnets, optimizing pole arc to pole pitch ratio (α), skewing the slots or magnets, and adding dummy slots [9]–[11]. Also, torque ripples are reduced by adopting different winding types. Among different shapes of magnets, trapezoidal-shaped PMs exhibit better performance as compared to the circular and rectangular-shaped PMs. An AFPM machine having arc-shaped trapezoidal PM was proposed in [12], where torque ripples were reduced as compared to the trapezoidal-shaped PM. However, using the arc-shaped trapezoidal PM, the back EMF was reduced too.

In this paper, an elliptical-trapezoidal-shaped PM AFPM machine is proposed to reduce the torque ripples and consequently enhance the output power and torque. By the use of elliptical-trapezoidal shape PM, an effective reduction of torque ripple and an improvement in back EMF is observed. To further reduce the torque ripple and increase in the back EMF, magnet overhang configuration is employed in proposed PM-shaped machine. The 3-D analysis of dual sided AFPM machine having elliptical trapezoidal-shaped magnets and drum winding on the stator is performed by using time stepped 3-D FEA. The results of AFPM machine having elliptical-trapezoidal PMs are compared to the conventional model. Furthermore, the optimization is performed by using genetic algorithm (GA). The results show a salient

Submitted On: July 16, 2019
Accepted On: July 6, 2021

https://doi.org/10.47037/2021.ACES.J.360819

reduction in the torque ripples and an increase in output torque.

II. COMPARISON BETWEEN PROPOSED AND THE CONVENTIONAL MODEL

The structure of slot-less AFPM machine consists of slotless iron stator sandwiched between the two rotor discs. Each rotor has surface mounted PMs of alternate magnetic polarity on it. Furthermore, Drum winding is used on the stator of AFPM machine in the middle of assembly. N-N type magnet configuration is used instead of N-S configuration because in drum winding the flux should flow through the stator core for maximum utilization of the windings.

Various PMs Shapes are used in AFPM machine for reducing torque ripples. However, trapezoidal-shaped PM for an AFPM machine provides better effective utilization of the rotor back iron surface as compared to the rectangular, sine wave, orthogonal and circular-shaped PMs. The increased effective utilization makes enhanced output torque. In addition, trapezoidal-shaped PM provides more uniform inter-polar separation between PMs along radial length of the disc which results in less cogging torque. AFPM machine with flat trapezoidal-shaped PMs and arc-shaped trapezoidal PMs are categorized as conventional-shaped and arc-shaped models, respectively. While an elliptical trapezoidal PM-shaped is proposed in this paper for the reduction of torque ripples.

Exploded view of elliptical trapezoidal double rotor slotless stator AFPM machine is shown in Fig. 1. Conventional, arc-shaped, and proposed models have flat top trapezoidal magnet, arc top trapezoidal magnet and elliptical trapezoidal magnet shapes, respectively. The design parameters of dual rotor single stator AFPM machine are listed in Table 1.

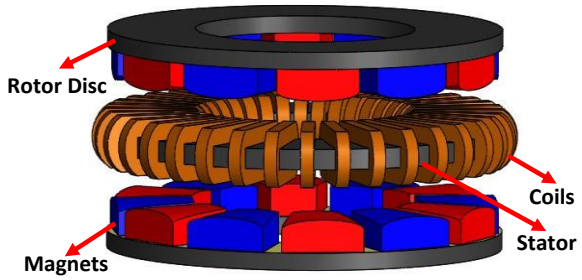

Fig. 1. Exploded view of slot-less AFPM machine.

Volume of PM in all three cases is kept constant. Height of inner and outer edge of flat top trapezoidal PM is same; however, it is different in the arc and elliptical top trapezoidal PMs as shown in Fig. 2.

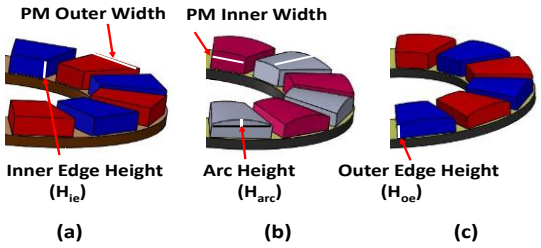

Fig. 2. Comparison of PM shapes: (a) flat trapezoidal, (b) arc trapezoidal, and (c) elliptical trapezoidal.

Table 1: Parameters of machines

Parameter	Value	Parameter	Value
Speed	1100 rpm	Stator yoke height	6.5 mm
Poles	12	Rotor yoke height	5.5 mm
Coils	36	Conductor size	0.71 mm
Air-gap	1 mm	$H_{ie\_conventional}$	10 mm
B_r	1.4 T	$H_{oe\_conventional}$	10 mm
L_m	30 mm	$H_{ie\_arc\ shape}$	9.1 mm
Coil height	16.7 mm	$H_{oe\_arc\ shape}$	7.64 mm
N_{ph}	420	$H_{ie\_proposed}$	8.7 mm
D_o/D_i	152/84.6	$H_{oe\_proposed}$	7 mm
α	0.8	$H_{arc\_arc\ shape}$	3 mm
Magnet volume	7433.1 mm^3	Coil resistance	0.1 ohm

In proposed elliptical top trapezoidal PM model, air-gap is larger than flat top trapezoidal PM model and smaller than arc top trapezoidal PM model. Comparison of air-gap lengths in flat, arc, and proposed elliptical top models is shown in the Fig. 3. Air-gap length l_g is constant and smaller in conventional flat trapezoidal PM shape due its flat top shape. The air-gap length l_g is largest in arc-shaped model and at intermediate sized in proposed elliptical model as ellipse is flatter than arc. However, there is a small difference of l_g in arc top and proposed elliptical model. Air-gap length comparison for various PM-shaped models is given in the following equation:

$$I_{g\_Arc\ shape} < I_{g\_Proposed} < I_{g\_Conventional}\ . \quad (1)$$

In conventional PM model, ϕ_g is greater than arc top and proposed elliptical model. Arc-shaped and proposed elliptical models have very minor difference of ϕ_g while arc-shaped model has the lowest value of ϕ_g. Air-gap flux comparison for the various PM shapes is given in the following equation:

$$\phi_{g\_Arc\ shape} < \phi_{g\_Proposed} < \phi_{g\_Conventional}\ . \quad (2)$$

$T_{cogging}$ is directly proportional to air-gap flux ϕ_g and the factor $dR/d\theta$ which is a change in air-gap reluctance with respect to change in the rotor position.

The relationship of cogging torque, air-gap flux, and air-gap reluctance is given as in the equation (3) [12]:

$$T_{cogging} = -\frac{1}{2}\phi_g^2 \frac{dR}{d\theta}, \quad (3)$$

where, ϕ_g is the air-gap flux, R is the air-gap reluctance, and θ is the position of rotor.

The change in the flux and change of reluctance is responsible for the cogging torque in any permanent magnet machine. Abrupt change in the reluctance is caused by the stator slots whereas the sharp edges of the magnet cause the sudden change in MMF and hence the air-gap flux to change abruptly. Air-gap flux change is smoother in elliptical magnet shape which results in less cogging torque.

The MMF is given by:

$$F_m = H_c l_m, \quad (4)$$

where F_m is the magneto-motive force, H_c is the magnetic field intensity and l_m is the height of magnet.

For flat top magnet l_m is same throughout the magnet and it has the sharp edges at both ends of magnet, which causes the sudden fall for MMF from a constant value but for arc-shaped and elliptical top magnet l_m changes gradually, *i.e.*, MMF is different at *a*, *b*, *c*, *d*, *e*, *f*, *g*, *h*, and *i*, points and MMF is reduced smoothly to the edges of the magnet.

Reduction of MMF in arc-shaped magnet causes EMF to reduce considerably because of sharp slope of l_m, from center of magnet to the edges.

The Elliptical top magnet is proposed as the solution of the problem because with the smoother surface, the l_m changes smoothly by a little value through point a, to point *i*, which causes the smaller change in MMF from point *a*, to point *i*, and hence the better distribution of air-gap flux with the less cogging torque and better EMF induction.

Figure (3) illustrates the different magnet shapes and the change in l_m for each magnet.

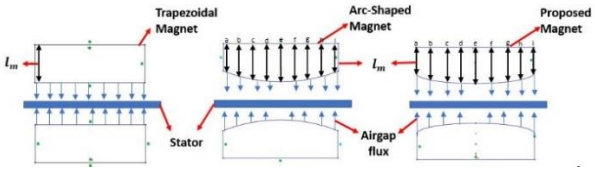

Fig. 3. Air-gap length comparison: (a) flat trapezoidal, (b) arc trapezoidal, and (c) elliptical trapezoidal.

A. Performance comparison of the conventional, arc, and proposed shape models

In this section, analysis of conventional flat trapezoidal PM model, arc trapezoidal PM model and proposed elliptical trapezoidal PM model is carried out by using 3-D finite element analysis (FEA). The results show that the proposed model has less $T_{cogging}$ as compared to the conventional and arc-shaped models. Furthermore, results show that proposed-shaped model results in increased back EMF as compared to the arc-shaped model.

The comparison of air-gap flux densities in conventional, arc-shaped, and proposed models is shown in Fig. 4. Results show that conventional model has the most and arc model has the least air-gap magnetic flux density. Air-gap flux density of proposed model lies between the air-gap flux densities of conventional and arc shape models.

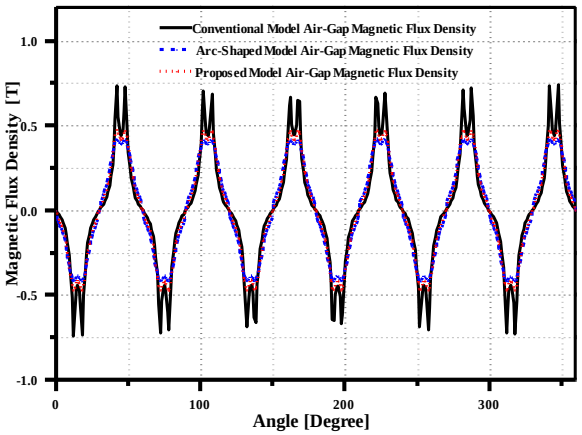

Fig. 4. Air-gap flux density comparison of conventional, arc shape and proposed model.

The comparison of cogging torque and back EMF for the conventional, arc-shaped, and proposed models a re made. The results show that cogging torque is maxim um in conventional model while minimum in proposed model. Also, the back EMF voltage is maximum in conventional and minimum in arc-shaped models. Comparison of cogging torque and back EMF for conve ntional, arc-shaped, and proposed models are shown in Figs. 5 and 6.

Conventional model has an average output power of 2208.5 W, whereas the average power the proposed and arc-shaped model is 2181W and 2108 W respectively, as shown in Fig. 7. Moreover, average output torque of conventional model is 22.82 Nm, arc-shaped model is 21.92 Nm, and the proposed model is 22.42 Nm. Furthermore, the Torque ripple in conventional, arc-shaped, and proposed model are 50.6%, 35.1% and 30.6%, respectively. Figure 8 shows the comparison of output torque of the conventional, arc-shaped, and proposed models.

The comparison of various performance parameters of conventional, arc-shaped, and proposed models is shown in Table 2.

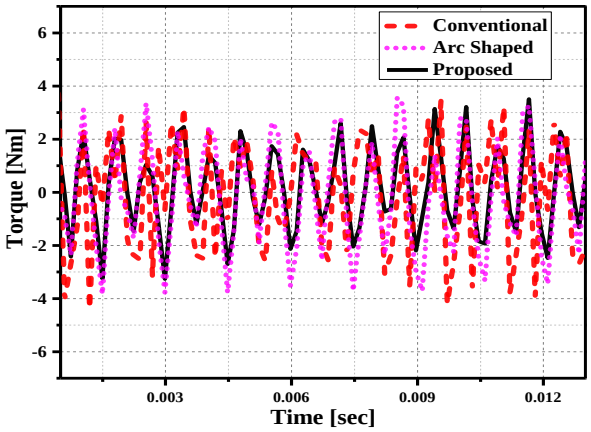

Fig. 5. Cogging torque comparison of conventional, arc shape and proposed model.

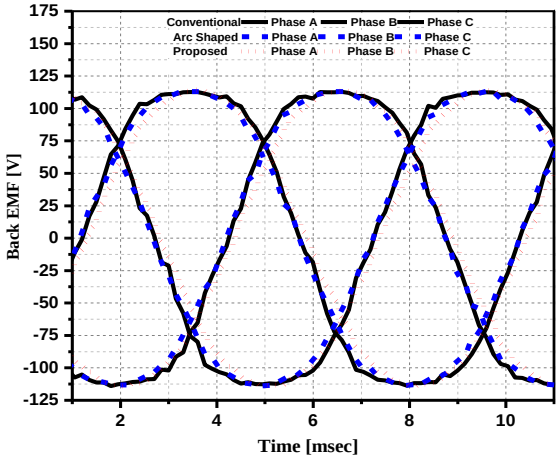

Fig. 6. Back EMF voltage comparison of conventional, arc shape and proposed model.

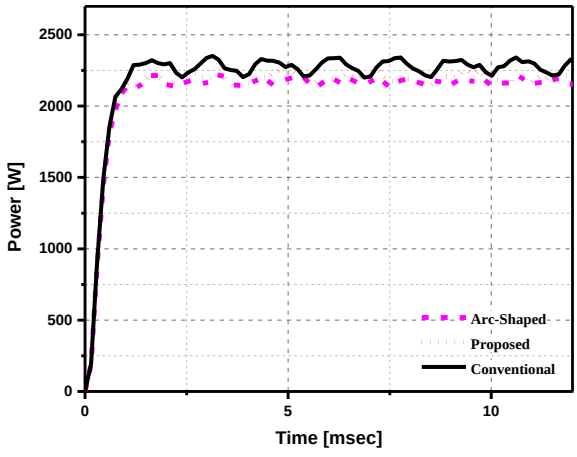

Fig. 7. Output power comparison of conventional, arc shape and proposed model.

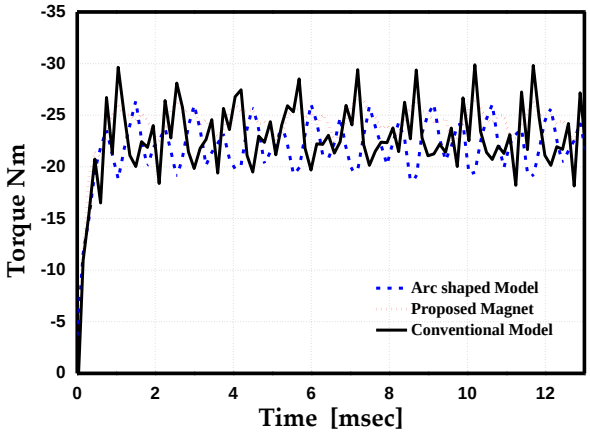

Fig. 8. Output torque comparison of conventional, arc shape and proposed model.

Table 2: Performance comparison of conventional, arc shape and proposed models

Parameters	Conventional Model	Arc-Shaped Model	Proposed Model
V_{rms}	87.6	83.1	84.4
$T_{cogging\ (pk2pk)}$	8.1	7.4	6.7
B_g (T)	0.335	0.282	0.293
V_{THD} (%)	12.2	5.6	8.8
1st & 3rd Harmonic	124.23, 12.04	118.19, 4.67	119.88, 6.7
τ_{avg} (Nm)	22.82	21.92	22.42
P_{avg} (W)	2208.5	2108	2181
$\tau_{ripples}$ (%)	50.6	35.1	30.6

III. OPTIMIZATION OF THE PROPOSED MODEL

A. Design variables

To increase the output torque as compared to the conventional model optimization of the proposed model is performed in this section.

Asymmetric magnet overhang is employed to optimize the proposed model and hence increase its back EMF and reduce the torque ripples. During optimization process, volume of elliptical trapezoidal PM is kept constant. Length of the magnet is varied along inner and outer radii by asymmetric overhang. Extending the magnet towards outer radii is termed as outer overhang and along inner radii is called inner overhang.

Latin Hypercube Sampling (LHS) was used get the samples of variables X_1, X_2 and X_3 from MATLAB. Total sixteen experiment were done with different values of parameters and the output EMF, and the cogging torque was analyzed. Genetic Algorithm (GA) was used to get the optimized value of the variables and the objectives. Values of variables and the Objectives is given in the Table 3.

Furthermore, magnet pole-arc to pole-pitch ratio and height of magnet are also varied. Height of PM is varied to make volume constant. Genetic algorithm (GA) is used to get the optimized results for average torque of proposed model. The limits of design variables are:

$$0\ mm < X_1 < 6.76mm,$$
$$0\ mm < X_2 < 8.5mm,$$
$$0.45 < X_3 < 0.8,$$

where X_1 the inner overhang of PM, X_2 is the outer overhang of PM, and X_3 the is pole-width to pole-pitch ratio (α).

According to the values of the variables X_1, X_2 and X_3, obtained by using Latin hyper cube sampling (LHS), trapezoid height of the magnet is varied to make the volume constant. Major axis of ellipse varies according to the width of the magnet and minor axis is fixed at 6 mm (3 mm half of ellipse). Pole pitch, width and height of PM are elaborated in Fig. 9.

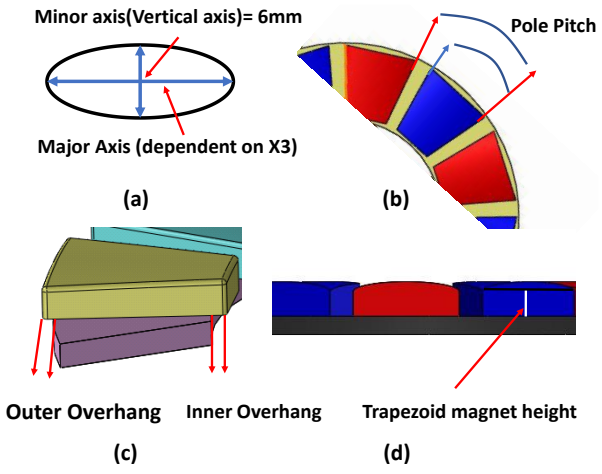

Fig. 9. Design variables of magnet.

Table 3: Experimental models for optimization and their results

No.	X_1	X_2	X_3	$T_{cogging}$	V_{rms}
1	6.03	6.16	0.54	7.34	87.51
2	3.55	5.72	0.76	6.75	89.91
3	0	1.76	0.56	6.70	80.01
4	0.35	6.6	0.63	7.46	88.77
5	5.68	4.84	0.62	5.66	88.99
6	1.42	8.36	0.47	10.01	68.19
7	6.39	7.92	0.78	5.31	90.35
8	2.84	7.48	0.74	7.79	91.04
9	3.90	3.08	0.8	7.46	89.85
10	1.06	3.52	0.58	6.49	82.46
11	5.32	1.32	0.73	3.36	87.47
12	4.97	2.64	0.65	7.21	87.01
13	2.13	2.2	0.69	8.65	87.47
14	1.77	3.96	0.51	9.33	80.74
15	6.74	7.04	0.67	7.50	89.90
16	2.48	0.88	0.45	8.25	72.17

B. Performance comparison after optimization

A comparison of various parameters for optimized elliptical-shaped permanent magnet machine with other machines is elaborated in this section. Flux density distribution of optimized elliptical-shaped permanent magnet model, conventional model and arc-shaped model is compared in Fig. 10. The optimization reduced maximum flux density from 1.8 T to 1.6 T. which shows significant improvement in the result.

The comparison of air-gap flux densities of conventional, arc-shaped, and optimized elliptical models using 3-D FEA analysis is shown in Fig. 11. The result shows a noticeable reduction in air-gap flux density.

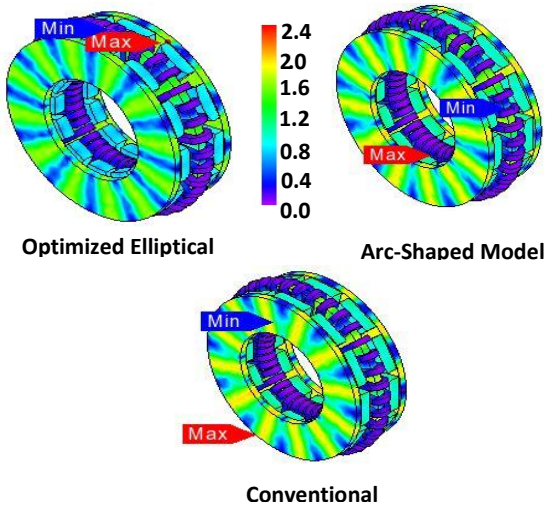

Fig. 10. Flux density distribution analysis of conventional, arc-shaped, and optimized elliptical models using 3D FEA.

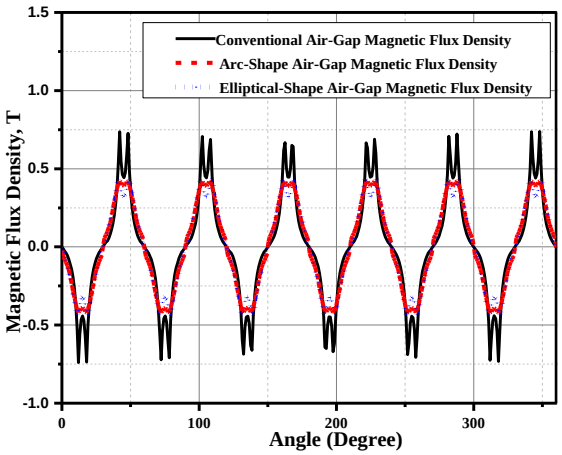

Fig. 11. Air-gap flux density comparison.

Figure 12 shows comparison of the back EMF of conventional, arc-shaped and optimized elliptical

models. The result shows that back EMF voltage is improved from 84.45 V_{rms} to 87.6 V_{rms} in elliptical-shaped model after optimization, which is an increment of 3.7 % in the back EMF of the model. Back EMF of conventional and arc-shaped model is 87.6 and 83.1, respectively.

The comparison of VTHD of conventional, arc-shaped and optimized elliptical models is made. Results show that the optimization improves the first harmonic from 119.88 V to 124.58 V as well as reduces the 3rd harmonic from 6.7 V to 2.23 V. Harmonic's comparison of conventional, arc-shaped and optimized elliptical models is shown in Fig. 13. VTHD is reduced from 8.8% to 4.3%. While VTHD in conventional and arc-shaped model is 12.2% and 5.6%, respectively.

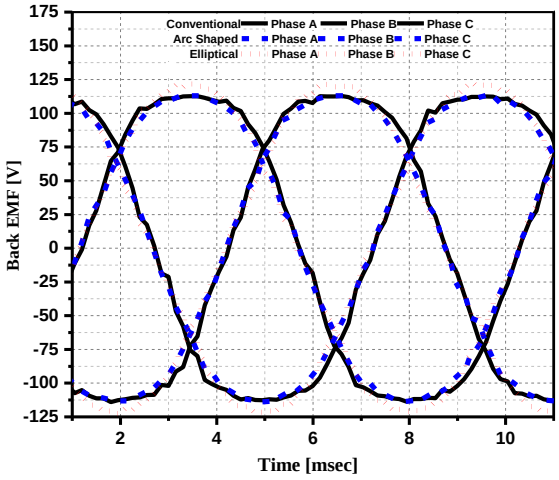

Fig. 12. Back EMF comparison.

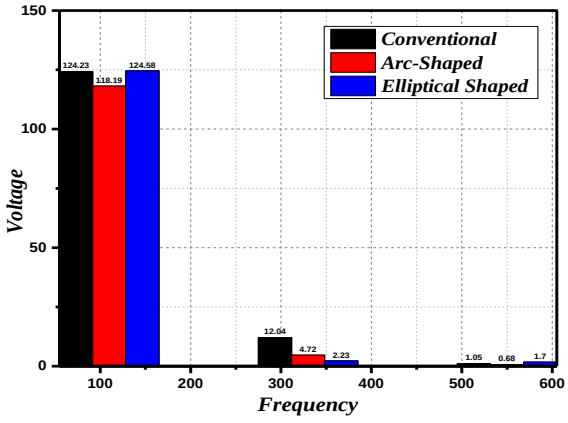

Fig. 13. Harmonics comparison.

Figure 14 shows comparison of the cogging torque for conventional, arc-shaped and optimized elliptical models. The peak-to-peak cogging torque of the proposed model is reduced from 6.77 Nm to 3.358 Nm, this shows a decrease of 50.4% through the optimization process. These results witnessed that cogging torque of the optimized model is further reduced while back EMF is also improved. So, the cogging torque of conventional, arc-shaped and optimized elliptical models is 8.1 Nm, 7.4 Nm, and 3.358 Nm, respectively.

A comparison of output power of conventional, arc-shaped and optimized elliptical models is made as shown in Fig. 15. The machine output power is improved by 7% after optimization from 2181.07 W to 2342.3 W, while output power of conventional model is 2208.5 W and that of arc-shaped model is 2108 W.

A comparison of output torque of conventional, arc-shaped and optimized elliptical models is made as shown in Fig. 16. After the optimization, output torque of the machine is improved by 7.8% and torque tipples are reduced to 17.58%. While torque ripples in arc-shaped and conventional models are 35.1% and 50.6% respectively.

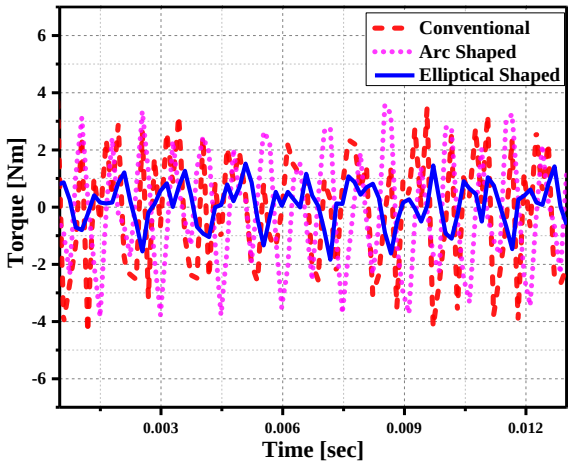

Fig. 14. Cogging torque comparison.

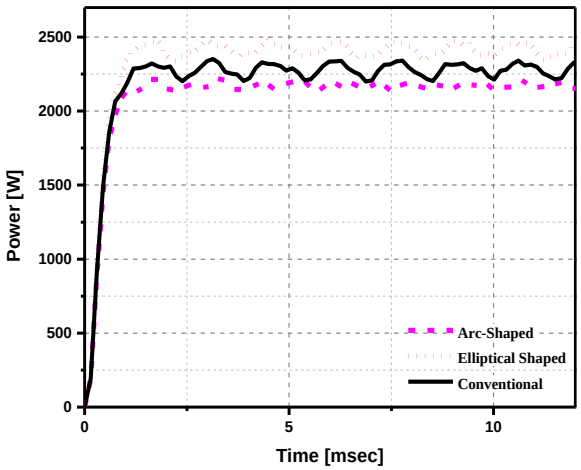

Fig. 15. Output power comparison.

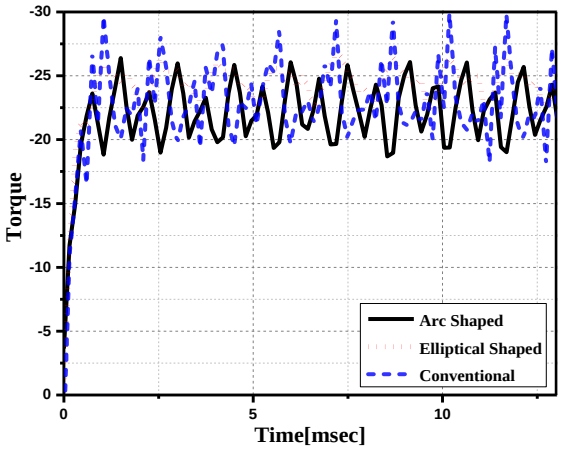

Fig. 16. Output torque comparison.

Performance comparison for proposed and optimized models is presented in Table 3. The results show that V_{rms} of optimized model is improved while $T_{cogging}$, VTHD and B_g (rms) is reduced in optimized model.

Table 3: Performance analysis of proposed and optimized model

Parameters	Elliptical Model	Conventional Model	Arc-Shaped Model
V_{rms}	87.6	87.6	83.1
$T_{cogging\ (pk2pk)}$	3.358	8.1	7.4
B_g (T)	0.282	0.335	0.282
V_{THD} (%)	4.3	12.2	5.6
1st & 3rd Harmonic	122.88, 2.23	124.23, 12.04	118.19, 4.67
τ_{avg} (Nm)	24.17	22.82	21.92
P_{avg} (W)	2342	2208.5	2108
$\tau_{ripples}$ (%)	17.58	50.6	35.1

IV. CONCLUSION

A model of the slotless AFPM machine using an elliptical trapezoidal-shaped PM is investigated in this paper. Proposed model has reduced cogging torque and torque ripples as compared to the conventional model. Furthermore, optimized elliptical-shaped magnet model has proved to be the most efficient model in terms of reduce cogging torque by an average of 58.54% as compared to the conventional model. Torque is also enhanced by 5.92% as the result of optimization of the proposed model as compared to the conventional model. Moreover, the decrease of 65.26% in torque ripples is also achieved. Additionally, power of AFPM generator is improved by 5.72%, from 2208 W to 2342 W. Hence, the optimal design demonstrates better performance as compared to the conventional and proposed models.

ACKNOWLEDGMENTS

This work was supported and funded by research and development department of Omnidex Group Limited, a multinational company with head office in 705, Building No. 7, Beijiaocheng Heng lu 1, Guangzhou 510050, P.R. China and article processing charge is supported by the Chung-Ang University Research Grant in 2020.

REFERENCES

[1] F. G. Capponi, G. De Donato, and F. Caricchi, "Recent advances in axial-flux permanent-magnet machine technology," *IEEE Trans. Ind. Appl*., vol. 48, no. 6, pp. 2190-2205, Nov./Dec. 2012.

[2] J. F. Gieras, R. Wang, and M. J. Kamper, Axial Flux Permanent Magnet Brushless Machines, *Dordrecht, The Netherlands: Kluwer*, 2004.

[3] A. Mahmoudi, S. Kahourzade, N. A. Rahim, W. P. Hew, and M. N. Uddin, "Design and prototyping of an optimised axial-flux permanent-magnet synchronous machine," *IET Electr. Power Appl*., vol. 7, no. 5, pp. 338-349, 2013.

[4] Y. P. Yang and D. S. Chuang, "Optimal design and control of a wheel motor for electric passenger cars," *IEEE Trans. Mag.*, vol. 43, no. 1, pp. 51-61, 2007.

[5] M. Andriollo, M. De Bortoli, G. Martinelli, A. Morini, and A. Tortella, "Permanent magnet axial flux disc generator for small wind turbines," *Proc. 18th Int. Conf. Electrical Machines*, pp. 1-6, 2008.

[6] P. K. Goel, B. Singh, S. S. Murthy, and S. K. Tiwari, "Three-phase four-wire autonomous wind energy conversion system using permanent magnet synchronous generator," *Electr. Power Compon. Syst.*, vol. 38, no. 4, pp. 367-386, 2010.

[7] S. Kahourzade, A. Mahmoudi, H. W. Ping, and M. N. Uddin, "A comprehensive review of axial-flux permanent-magnet machines," *Can. J. Elect. Comput. Eng*., vol. 37, no. 1, pp. 19-33, 2014.

[8] S. Wu, S. Zuo, X. Wu, F. Lin, and J. Shen, "Magnet modification to reduce pulsating torque for axial flux permanent magnet synchronous machines," *Applied Computational Electromagnets Society Journal*, vol. 31, no. 3, Mar. 2016.

[9] N. P. Gargov, A. F. Zobaa, and I. Pisica, "Investigation of multi-phase tubular permanent magnet linear generator for wave energy converters," *Electr. Power Compon. Syst.*, vol. 42, no. 2, pp. 124-131, 2014.

[10] E. Aycicek, N. Bekiroglu, I. Senol, and Y. Oner, "Rotor configuration for cogging torque minimization of the open-slot structured axial flux permanent magnet synchrnous motors," *Applied Computational Electromagnets Society Journal*, vol. 30, no. 4, pp. 396-408, 2015.

[11] T. M. Jahns and W. L. Soong, "Pulsating torque minimization techniques for permanent magnet ac motor drives: A review," *IEEE Trans. Ind. Electron*., vol. 43, no. 2, pp. 321-330, Apr. 1996.

[12] J. Ikram, N. Khan, Q. Junaid, S. Khaliq, and B. I. Kwon, "Analysis and optimization of the axial flux permanent magnet synchronous generator using an analytical method," *Journal of Magnetics*, vol. 22, pp. 257-265, 2017.

[13] K. Y. Hwang, H. Lin,S. H. Rhyu, and B. I. Kwon, "A study on the novel coefficient modeling for a skew permanent magnet and overhang structure for optimal design of BLDC motor," *IEEE Transactions on Magnetics*, vol. 50, pp. 1918-1923, 2012.

Salman Ali was born in Pakistan on 1st April 1992. Ali received his B.S. degree in Electrical Engineering from Federal Urdu University Islamabad in 2015 and the M.S. degree in Electrical Engineering from COMSATS University Islamabad in 2019. He was Research Associate in COMSATS University from 2017 to 2019. Currently, He is serving as Electro-Mechanical Development Engineer in R&D Department of Omnidex Group Limited since 2019. His research interests are design, analysis and prototyping different topologies of electrical machines. Until now, most of his research is in the design, analysis, and prototyping of axial flux permanent magnet machines.

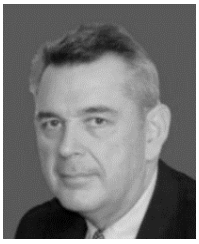

Christopher P. Devereux was born in England in 1947 but spent the next 4 years of his early life in Abbottabad, Pakistan. On returning to England Christopher Devereux progressed through an uneventful British schooling until 17 when he organized and led an expedition into the Amazonas of Brazil. This inspired him to start a lifetime of travel basing himself first in Central and South America, then back to the UK and then on to China where he started and now runs an engineering company. He follows in his grandfather's footsteps (who filed over 200 engineering patents for the Indian railway system) in developing new engineering concepts and is the holder, himself, of several patents.

Syed Sabir Hussain Bukhari received his B.E degree in Electrical Engineering from Mehran University of Engineering and Technology Jamshoro, Pakistan, in 2009, and Ph.D. from the Department of Electronic Systems Engineering, Hanyang University, South Korea in 2017. He joined Sukkur IBA University as an Assistant Professor in December 2016. He is currently working as a Research Professor at Chung-Ang University, Seoul, South Korea under Korean Research Fellowship (KRF) program. His main research interests include electric machine design, power quality, and drive controls.

Junaid Ikram received his B.E. degree in Electrical Engineering from University of Engineering and Technology Lahore, Pakistan in 2005, M.S. degree from Hanyang University, South Korea in 2009 and he did his Ph.D. degree in Electrical Engineering from Comsats University Islamabad, Pakistan in 2017. Currently he is working as a Senior Engineer in COMSATS University Islamabad. His research interests include design, analysis and optimization of axial flux machines, vernier machines, wound rotor synchronous machine, hybrid flux switching machines and modeling of the machine losses.

Shahid A. Khan received the B.S. degree in Electrical Engineering from the University of Engineering and Technology, Lahore, Pakistan, and the M.S. and Ph.D. degrees in Radio Communications from the Universality of Portsmouth, U.K. In 2003, he joined COMSATS University Islamabad (CUI) as an Assistant Professor and elevated to a professor within few years. He worked as the HOD, the Chairman, and the Dean of the Faculty of Engineering. He is currently the Founder of various engineering programs in different campuses of CIIT. He has established many teaching and research labs by securing funding of about ten million USD. He has authored over 80 research articles published in international journals and conferences. On the basis of his meritorious services, he has been honored with multiple awards and memberships in the field of engineering education.

Nasrullah Khan received the B.Sc. degree in Electrical Engineering degree from UET Lahore, in 1984, the M.Sc. degree from Reading University, U.K., in 1988, and the Ph.D. degree from Essex University, U.K., in 1992. He has 21 years teaching and research and 12 years practical field experience. He has done several research projects in COMSATS and abroad. He has 34 years local and foreign teaching, research, and field experience.

Jong-Suk Ro received the B.S. degree in Mechanical Engineering from the Han-Yang University, Seoul, South Korea, in 2001, and the Ph.D. degree in Electrical Engineering from Seoul National University (SNU), Seoul, South Korea, in 2008. He conducted research at the Research and Development Center of Samsung Electronics as a Senior Engineer, from 2008 to 2012. From 2012 to 2013, he was with the Brain Korea 21 Information Technology of SNU, as a Postdoctoral Fellow. He conducted research at the Electrical Energy Conversion System Research Division, Korea Electrical Engineering and Science Research Institute, as a Researcher, in 2013. From 2013 to 2016, he worked with the Brain Korea 21 Plus, SNU, as a BK Assistant Professor. In 2014, he was with the University of Bath, Bath, U.K. He is currently an Associate Professor with the School of Electrical and Electronics Engineering, Chung-Ang University, Seoul, South Korea. His research interests include the analysis and optimal design of next-generation electrical machines using smart materials such as electromagnet, piezoelectric, and magnetic shape memory alloy.